Hybrid clay-based materials for organic dyes and pesticides elimination in water

Marlène Huguette Tsaffo Mbognou [1,2,3], Stéphanie D. Lambert[1], Joachim Caucheteux[1], Antoine Farcy[1], Christelle Alié[1], Nathalie Fagel[4], Emmanuel Djoufac Woumfo[2], Julien G. Mahy [1,5,*]

[1] Department of Chemical Engineering – Nanomaterials, Catalysis & Electrochemistry, University of Liège, B6a, Quartier Agora, Allée du six Août 11, 4000 Liège, Belgium.

[2] Laboratoire de Physico-chimie des matériaux minéraux, University of Yaounde I, 337 Yaounde, Cameroon.

[3] Institute of Geological and Mining Research (IRGM),4110 Yaounde, Cameroon

[4] Laboratoire Argiles, Géochimie et Environnements sédimentaires (AGEs), Department of Geology, Faculty of Sciences, University of Liège, Liège, B-4000, Belgium;

[5] Institut National de la Recherche Scientifique (INRS), Centre-Eau Terre Environnement, Université du Québec, 490, Rue de la Couronne, Québec (QC), G1K 9A9, Canada

*Corresponding author: Julien G. Mahy; email: julien.mahy@uliege.be ; address: Allée du Six Août 11, 4000 Liège, Belgium

Abstract

Natural clay, extracted from Cameroon, was modified by ion exchange to produce 4 different clays. These latter were modified with photocatalytic semiconductor like ZnO to produce efficient hybrid materials for pollutant removal in water. ZnO was synthesized by the soft sol-gel chemistry method.

The results showed that the clay belonged to the smectite family and was composed of different crystalline phases. When the hybrid materials were produced, mix crystalline patterns were obtained with both smectite and ZnO wurtzite phases. The ICP-AES analysis showed that similar ratio between ZnO and clay were obtained for the 4 hybrid materials (30 wt% of ZnO and 70 wt% of clay). The SEM observation of the samples had shown that the hybrid materials had the clay structure as skeletal structure (sheet like structure) with the ZnO spherical materials grafted at the surface, giving a good exposure to light to maintain photocatalytic property.

Then, the pollutant removal property of the samples was evaluated on three different model pollutants: p-nitrophenol (PNP), Malachite green (MG) and Diamant brilliant violet (DBV). On PNP, no

adsorption was observed, and photocatalytic property was necessary to eliminate this molecule. With the best hybrid material (Clay/Cu^{2+}/ZnO), 80% of PNP degradation was observed after 6 h of illumination. On MG and DBV, similar behavior was observed. Indeed, the clays and three out of four hybrid materials adsorbed completely both pollutant after 2 h of contact. Only pure ZnO and Clay/ZnO needed illumination to degrade completely both molecules. This study showed the possibility to obtain very efficient hybrid materials for pollutant removal in water with the use of inexpensive natural clay modified with a low amount of photocatalytic material (ZnO around 30 wt.%).

Keywords : Adsorption, Photocatalysis, Smectite, ZnO, Green chemistry, Sol-gel

1. Introduction

In recent decades, environmental pollution by the excessive presence of bio-refractory organic pollutants in wastewater from domestic uses or industries is a serious environmental scourge [1]. Some of these compounds are recognized as capable of causing carcinogenic and mutagenic effects and interfering with the hormonal system of living beings. Among the pollutants commonly detected in industrial discharges are organic dyes, organochlorines, phenolic compounds, etc [2]. These compounds are the cause of numerous disturbances of aquatic fauna and constitute a risk for human health [3]. Faced with this situation, several countries have been forced to set strict legislative and normative constraints towards manufacturers for the protection of the environment. Thus, the major challenge for industries is to find an effective and inexpensive technique to reduce the level of pollution to the threshold accepted by the legislation before any discharge into the environment. Attention was subsequently focused on the use of new adsorbents based on abundant natural materials. This is the case for clays [4]. As a raw material, clay is a mixture of clay minerals and crystalline impurities in the

form of rock debris of infinitely diverse compositions. The interest given in recent years to the study of clays by many laboratories around the world [5] is justified by their abundance in nature, the importance of the specific surfaces they develop [6], the presence of surface charges and especially the exchangeability of the interfoliar cations. The latter, also called mobile or compensating cations, are the main elements responsible for hydration, swelling and plasticity, and they give these clays hydrophilic properties. Existing conventional techniques such as adsorption, coagulation/flocculation, and biological treatment are increasingly ineffective in the face of the complexity of effluents [7]. Moreover, these techniques require an additional investment, for the treatment of liquid/solid concentrate formed.

To overcome these problems, efficient and ecological treatment strategies have been developed. Among which is the application of advanced oxidation processes (AOPs), which are based on the production of hydroxyl radicals, very reactive and strongly oxidizing species. These processes include heterogeneous photocatalysis under UV and/or visible light [8–11], homogeneous phase chemical oxidation processes: H_2O_2/Fe^{2+} (Fenton's reagent) [12], O_3/OH^- (ozonation) [13]; photochemical processes: UV only, H_2O_2/UV, O_3/UV, H_2O_2/Fe^{3+}/UV (photo-Fenton) [12, 14]; electrochemical processes [15, 16] (anodic oxidation, electro-Fenton) etc... However, although effective for the mineralization of most organic pollutants, these processes require an external energy input (electric or magnetic) and consequently a relatively high cost for a strong mineralization of the pollutant. Hybrid materials having multiple pollutant removal properties can be of great interest to treat this pollution [17–19].

In this work, the main goal is to produce hybrid materials made of good adsorbent materials (clay) and efficient photocatalyst (ZnO) at low price. Indeed, the goal is to develop a hybrid material that can depollute water either with adsorption or photocatalytic processes. To reach this goal, natural clay extract from Cameroon will be used and also modified by ion exchange process to increase their adsorption properties. The ZnO, introduced in clay, is synthesized by a green sol-gel process and the amount added in the hybrid material is limited to 30 wt.% to conserve low prices for these materials.

The hybrid materials and the corresponding pure clay and pure ZnO samples are characterized to determine their composition and morphology. Then, the pollutant removal property of these samples is evaluated on model water polluted with three different molecules: the *p*-nitrophenol (PNP), the malachite green (MG) and the Diamant brilliant violet (DBV). PNP and MG are commonly found in pesticide [20, 21] and MG and DBV are used as organic dye [21, 22].

2. Materials and Methods

2.1. Natural Clays

Natural clays were extracted from Bana in Cameroon, details were given in [23]. After extraction, the clays were dried to a constant weight. Then some part was modified to insert Cu^{2+}, Na^{+} or Zn^{2+} ions.

Copper ions insertion

The protocol is detail in [23] and summarized below.

The reagents used are the following: copper (II) sulfate pentahydrate (> 98.0%, Sigma-Aldrich), barium sulfate (99%, Sigma-Aldrich), clay powder (> 160 µm), distilled water [23].

In order to produce a homogeneous cation exchange, 50 g of clay was mixed under stirring in 0.1 M of $CuSO_4$ solution for 4 h. After 2 h at rest, the supernatant was poured, and the agitation was repeated with a new solution of 0.1 M of $CuSO_4$. This operation was repeated twice, and excess Cu^{2+} and SO_4^{2-} ions were washed with distilled water until the Baryum test (precipitation test) became negative. The homoionic Cu^{2+} clay material was then oven dried at 110 °C overnight [23].

Sodium ions insertion

The reagents used are the following: distilled water, sodium chloride (Dry Basis >99.5%, Fisher BioReagents), silver nitrate (99%, extra pure, Laboratorium discounter), clay powder (> 160 µm).

Sodium homo-ionization allows to replace all exchangeable cations of various natures by only sodium cations. 100 g of clay material are treated with magnetic stirring for 72 h by a solution of NaCl 1M. The material is dried at 100 °C for 24 h.

To ensure that the cation exchange reaction was effective, the dispersion of clay in the electrolyte solution was maintained under stirring for 4 h. After settling, the supernatant is removed, and the recovered solid is re-dispersed in the renewed salt solution. This operation has been repeated 4 times in order to achieve a complete cation exchange with Na^+ ions. The excess of Na^+ and Cl^- ions were washed with distilled water until the silver nitrate test (precipitation test) became negative. Indeed, when solution containing Cl^- ions is in contact with $AgNO_3$, a precipitate appears. If the test is negative, it proves that all Cl^- ions have been removed from the sample thanks to the washing step.

Zinc ions insertion

This treatment does not destroy the structure of the clay material and it allows the insertion of Zn ions. We used the following reagents: zinc (II) chloride (> 97.0%, Laboratorium discounter), silver nitrate (99%, extra pure, Laboratorium discounter), clay powder (> 160 µm), and distilled water. In order to produce a homogeneous cation exchange, 50 g of clay was mixed under stirring in 0.1 M of $ZnCl_2$ solution for 4 h. After 2 h at rest, the supernatant was poured, and the agitation was repeated with a new solution of 0.1 M of $ZnCl_2$. This operation was repeated twice, and excess Zn^{2+} and Cl^- ions were washed with distilled water until the silver nitrate test (precipitation test) became negative. Indeed, when solution containing Cl^- ions is in contact with $AgNO_3$, a precipitate appears. If the test is negative, it proves that all Cl^- ions have been removed from the sample thanks to the washing step. The homoionic Zn^{2+} clay material was then oven-dried at 100 °C overnight.

2.2. ZnO synthesis

Pure zinc oxide powders were synthesized by the sol-gel method following Benhebal *et al.* [24, 25]. The reagents were zinc acetate dihydrate (≥ 98%), oxalic acid dihydrate (≥ 99%), and absolute ethanol (ACS grade). They were obtained from BIOCHEM, Chemopharma (Cosne-Cours-sur-Loire, France), of analytical grade, and used directly as purchased.

Zinc acetate dihydrate (10.98 g) was treated with ethanol (300 mL) at 60 °C. The salt was completely dissolved in about 30 min. Oxalic acid dihydrate (12.6 g) was dissolved in ethanol (200 mL) at 60 °C for 30 min. The oxalic acid solution was added slowly, with stirring, to the hot ethanolic zinc solution, and the mixture was stirred for 90 min at 50 °C. The resulting gel was placed in an oven at 80 °C for 24 h. The product was calcined at 500 °C for 3h.

2.3. Hybrid Clay-ZnO materials synthesis

For the preparation of hybrid clays with ZnO, the procedure was similar as for pure ZnO material. However, when the oxalic acid solution was added slowly with stirring to the hot ethanolic zinc solution, 10 g of doped clay materials was added, and the mixture was left under stirring for 90 min at 50 °C. The resulting gel was placed in an oven at 80 °C for 24 h. The product was calcined at 500 °C for 3 h. The ZnO-modified clay powders were light gray in color.

2.4. Characterizations

Samples were measured by nitrogen adsorption desorption isotherms in an ASAP multisampler device from Micromeritics.

The actual composition of the natural and hybrid clays was determined by inductively coupled plasma–atomic emission spectroscopy (ICP–AES), equipped with an ICAP 6500 THERMO Scientific device (Waltham, MA, USA). The mineralization is fully described in [26]; however, we used HF instead of HNO_3.

X-ray diffraction patterns were recorder on a Bruker D8 Twin-Twin powder diffractometer (Bruker, Billerica, MA, USA) using Cu-K_α radiation.

Scanning electron microscopy pictures were obtained on a TESCAN CLARA microscope operating at 15 keV.

2.5. Photocatalytic and adsorption experiments

The degradations of *p*-nitrophenol (PNP), Malachite Green (MG) and Diamant Brilliant Violet (DBV) were studied under UVA light (λ = 365 nm) to determine the photocatalytic activity of the synthesized material. The lamp was an Osram Sylvania, Blacklight-Bleu Lamp, F 18W/BLB-T8, with its maximum peak at 365 nm and an intensity of 1.2 mW/cm^2.

Each sample was placed in a Petri dish with 20 mL of the pollutant solution in water (14 mg/L for PNP, 4 mg/L for MG or DBV). The degradation of the pollutant was evaluated from absorbance measurements with a Genesys 10S UV-Vis spectrophotometer (Thermo Scientific). Previously, adsorption tests were performed in the dark (dark tests) to show whether the pollutant was adsorbed on the surface of samples. A blank test, consisting of irradiating the pollutant solution for 24 h in a Petri dish without any catalyst, is made to assess the photolysis of the three pollutants under this illumination. The Petri dishes with catalysts and pollutants were stirred on orbital shakers (90 RPM) and illuminated for 24 h. Aliquots of pollutant were sampled at 0, 2, 6 and 24 h. The photocatalytic degradation can be evaluated by taking the catalyst adsorption (dark test) into account. Each photocatalytic measurement was triplicated to assess the reproducibility of the data. In each box, the

catalyst concentration was equal to 1 g/L. Another experiment was also done with a catalyst concentration of 0.3 g/L only for the pure ZnO sample, in order to have the same amount of photocatalyst as the hybrid materials which contain 30 wt.% of ZnO.

The same experiments without light were performed to assess the adsorption properties of the samples on the three different model pollutants.

3. Results and Discussion

3.1. Composition and morphologies of the clay-based materials

Table 1 gives the composition of the different samples. The bare Clay and the ion modified Clays have similar compositions with a Si/Al ratio around 2, characteristic ratio of smectite [27]. The ion modified clays have respectively higher amounts of the ion which was added during the modification process as expected.

For the ZnO/Clay hybrid materials, the Si/Al ratio stay equal around 2 and the proportion of ZnO is around 30 wt.% for each of the 4 hybrid materials as expected.

Table 1: Sample composition given by ICP-AES.

Samples	Al (wt.%)	Si (wt.%)	Na (wt.%)	Cu (wt.%)	Zn (wt.%) [and ZnO (wt.%)]
Bare Clay	10.1	20.9	<0.1	<0.1	<0.1
Clay/Na^+	10.2	20.9	0.2	<0.1	<0.1
Clay/Cu^{2+}	11.5	21.2	<0.1	0.8	<0.1
Clay/Zn^{2+}	10.5	21.4	<0.1	<0.1	2.1
Pure ZnO	-	-	-	-	>99
Clay/ZnO	5.2	9.2	<0.1	<0.1	18.9 [28.1]
Clay/Na^+/ZnO	5.8	10.3	0.1	<0.1	23.0 [29.0]
Clay/Cu^{2+}/ZnO	6.4	11.6	<0.1	0.4	23.3 [30.3]
Clay/Zn^{2+}/ZnO	6.0	11.7	<0.1	<0.1	26 [31.2]

XRD patterns allow to estimate the crystalline phase presented in the samples, the patterns are represented in Figure 1 for all samples.

For the 4 clays (bare Clay, Clay/Cu^{2+}, Clay/Na^{+}, and Clay/Zn^{2+} samples), similar patterns are observed with several crystalline phases that are pointed on bare Clay pattern. These patterns correspond to the smectite family which encompasses the different phases observed *i.e.* augite, cristobalite, montmorillonite, illite, kaolinite, feldspar, and talc. The pure ZnO sample (in green) is composed of wurtzite phase (peaks denoted as Z) as expected.

When hybrid materials are formed (Clay/ZnO, Clay/Cu^{2+}/ZnO, Clay/Na^{+}/ZnO, and Clay/Zn^{2+}/ZnO samples), the patterns correspond to a mix of the initial Clay pattern with the wurtzite peaks, showing that the hybrid materials are successfully obtained.

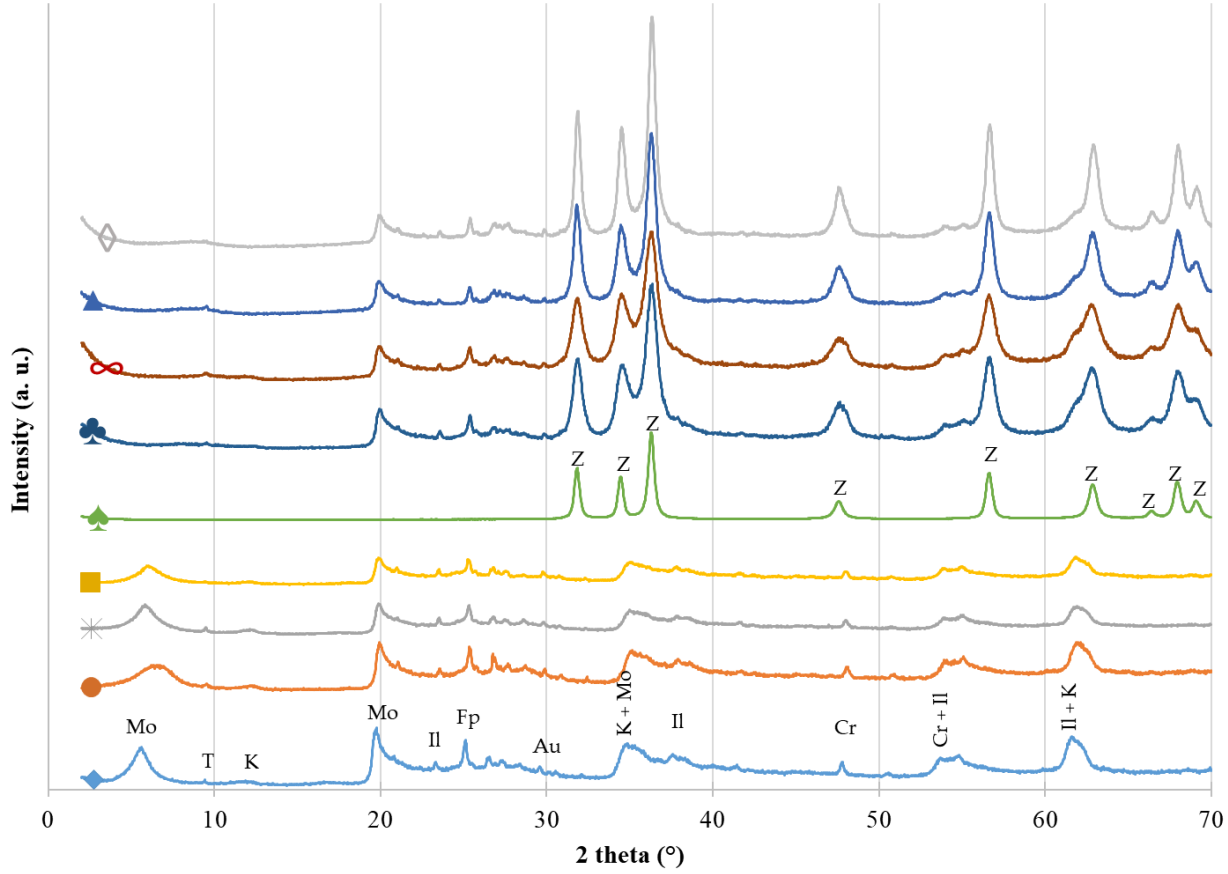

Figure 1: XRD patterns of samples: (♦) bare Clay, (●) Clay/Cu^{2+}, (*) Clay/Na^{+}, (■) Clay/Zn^{2+}, (♠) Pure ZnO, (♣) Clay/ZnO, (∞) Clay/Cu^{2+}/ZnO, (▲) Clay/Na^{+}/ZnO,and (◊) Clay/Zn^{2+}/ZnO. The positions of the reference peaks are indicated on the two pure materials (bare Clay and ZnO) by the following letters: (Z) Wurzite, (Mo) Montmorillonite, (T) Talc, (K) Kaolinite, (Il) Illite, (Fp) Feldspath, (Au) Augite

and (Cr) Cristobalite. The positions are not indicated on the composites materials to not overload the figure.

Table 2 presents the specific surface area and the porous volume (V_p) for the different samples. The specific surface values are slightly increased when ions are inserted in the clay network. Indeed, the specific surface area increases from 45 m^2/g to 50-55 m^2/g when cations are inserted (Table 2). An increase is also noted for the pore volume. Concerning the pure ZnO material, a specific surface value of 30 m^2/g is obtained. When the clay is modified with ZnO, a slight increase is observed for all the modified samples. Concerning the pore volume, an increase is also observed for all samples (Table 2). Indeed, the grafting of the ZnO particles at the surface of the sheets of clay (explained in the next paragraph and observed on the SEM images in Figure 3) produces a rougher surface with more pore volume. Figure 2 gives an example of the isotherms that are obtained for Clay/Zn^{2+} and Clay/Zn^{2+}/ZnO samples and that are very similar for each sample. These isotherms correspond mainly to the type IV isotherm characterized by a broad hysteresis at high pressure (mesoporous solid).

Table 2: Specific surface area and porous volume.

Samples	Specific surface area (m^2/g) ± 5	V_p (cm^3/g) ± 0.01
Bare Clay	45	0.07
Clay/Na^+	50	0.08
Clay/Cu^{2+}	55	0.09
Clay/Zn^{2+}	50	0.09
Pure ZnO	30	0.14
Clay/ZnO	60	0.44
Clay/Na^+/ZnO	55	0.25
Clay/Cu^{2+}/ZnO	50	0.21
Clay/Zn^{2+}/ZnO	50	0.18

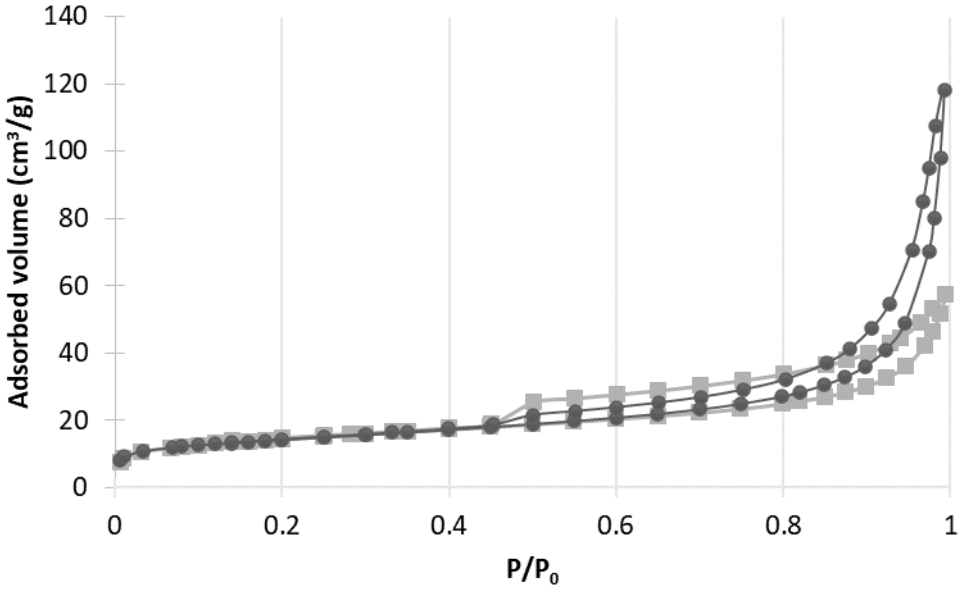

Figure 2: Nitrogen adsorption–desorption isotherms for (■) Clay/Zn^{2+} and (●) Clay/Zn^{2+}/ZnO samples.

Figure 3 gives an overview of the 9 samples observed by SEM. For the 4 clays ((a) bare Clay, (b) Clay/Cu^{2+}, (c) Clay/Na^{+}, and (d) Clay/Zn^{2+} samples), sheet like materials are observed as expected for clay materials [28, 29], with smooth surface. No difference in the samples is noted.

When hybrid material is formed (Figure 3f to 3i), the sheet like structure is still observed but rough surfaces are observed with the presence of sphere materials covering the surface. These spheres correspond to the ZnO material as it is observed on the pure ZnO sample in Figure 3e. So the hybrid material is composed of the clay as bone structure covered by ZnO particles. It is important for the photocatalytic properties that the ZnO particles are present at the surface to be in contact with the light.

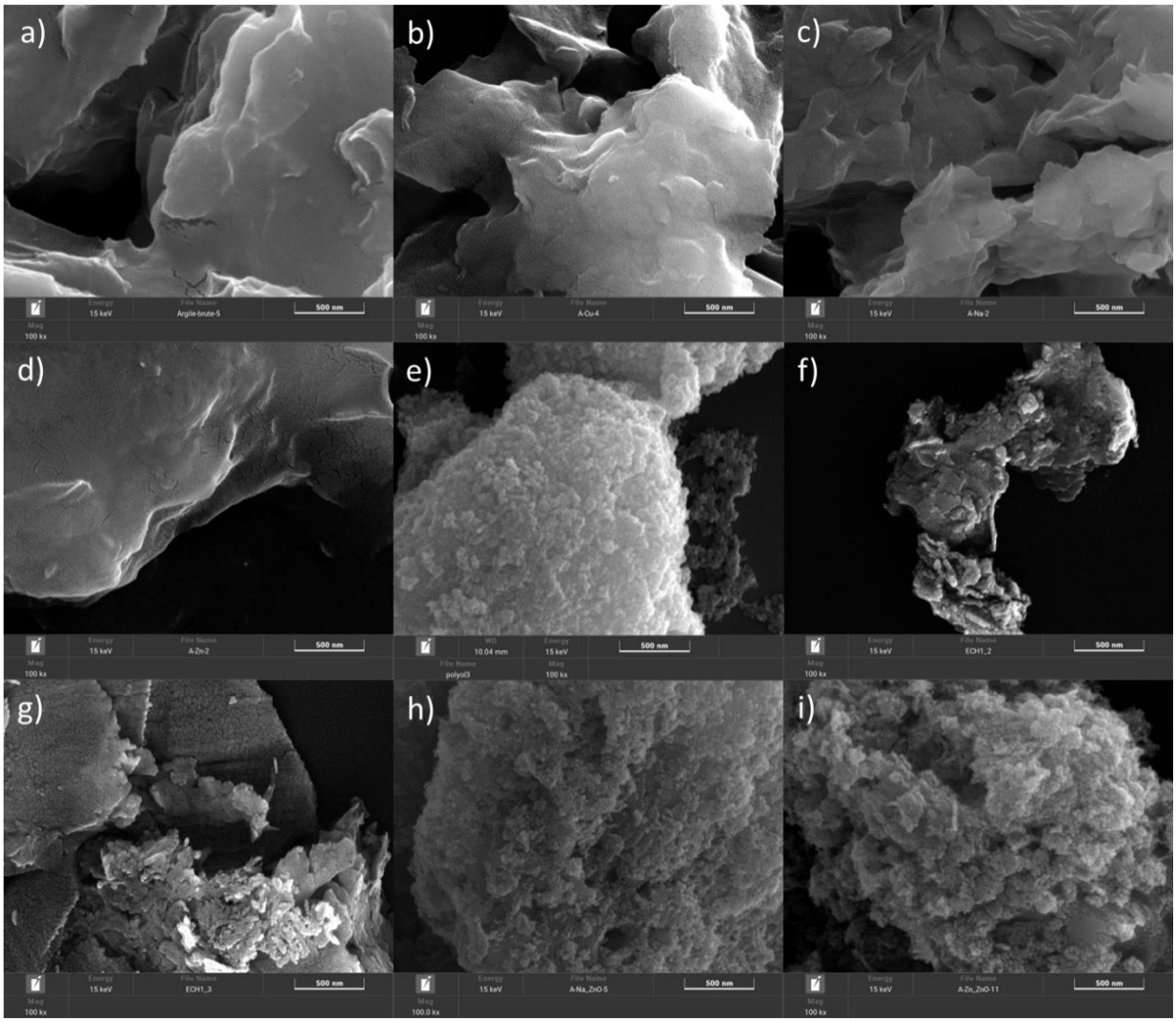

Figure 3: SEM pictures of samples: (a) bare Clay, (b) Clay/Cu^{2+}, (c) Clay/Na^{+}, (d) Clay/Zn^{2+}, (e) Pure ZnO, (f) Clay/ZnO, (g) Clay/Cu^{2+}/ZnO, (h) Clay/Na^{+}/ZnO, and (i) Clay/Zn^{2+}/ZnO.

Hybrid materials are successfully obtained composed of 30 wt.% of ZnO and 70 wt.% of clay, with the ZnO particles present at the surface.

3.2. Photocatalytic activity and adsorption property on three different pollutants

239 The materials are evaluated for pollutant removal via two processes: the adsorption and the
240 photocatalytic degradation. Their efficiencies are estimated on three different pollutants to show
241 versatility. Firstly, the blank test showed that the 3 pollutant concentrations under UVA illumination
242 remained constant and that no photolysis occurs.
243 The first pollutant to eliminate is the PNP, commonly found in pesticide. The results are presented on
244 Figure 4. First, during the experiments of adsorption made in the dark, no adsorption on any of the 9
245 samples was observed, so the adsorption results are not represented on Figure 4.
246 Also on Figure 4, the photocatalytic degradation of the PNP is presented after 2, 6 and 24 h of
247 illumination for the 9 samples, the pure ZnO sample is tested with two concentrations: 1 g/L and 0.3
248 g/L. Indeed, the concentration at 1 g/L is to have the same mass as the other samples and the
249 concentration of 0.3 g/L is to have the same amount of photocatalyst as the hybrid samples, which are
250 made of 30 wt.% of ZnO. For the 4 clays (bare Clay, Clay/Cu^{2+}, Clay/Na^{+}, and Clay/Zn^{2+} samples), no
251 degradation is observed as clay alone is not a photocatalytic material. As previously reported [23, 24,
252 30], pure ZnO (at 1 g/L) degrades PNP with an efficiency equal to 95 % after 6 h as ZnO is a
253 photocatalytic material active under UV-A illumination. When the concentration of ZnO is decreased
254 to 0.3 g/L, the degradation rate decreases also, reaching only 30 % after 6 h. When hybrid materials
255 are formed (Clay/ZnO, Clay/Cu^{2+}/ZnO, Clay/Na^{+}/ZnO, and Clay/Zn^{2+}/ZnO samples), photocatalytic
256 degradation of PNP is still observed for each hybrid material. Between the 4 hybrid materials, the three
257 one modified with ions present higher degradation that Clay/ZnO sample. Indeed, the presence of
258 these ions can increase the photocatalytic activity via photo-Fenton reactions for Cu^{2+} and Zn^{2+} [26, 31,
259 32]. For Na^{+}, it was reported that if Na^{+} doped the ZnO, it can increase its photocatalytic properties
260 [33]. The degradation of the hybrid materials is higher than the ZnO at the concentration of 0.3 g/L, it
261 can be explained by the specific morphology observed with SEM (Figure 3) showing that the ZnO
262 particles are distributed at the surface of clay sheet allowing a very good contact between the pollutant
263 and the photocatalytic material.
264

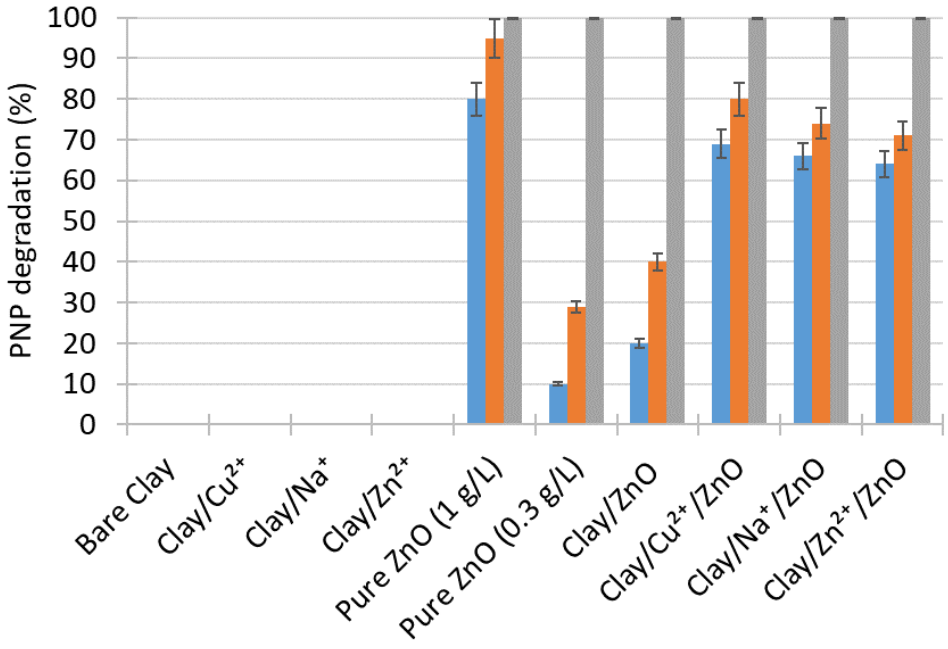

Figure 4: PNP degradation (%) under UVA illumination for 2, 6, and 24 h with all samples. (blue) = after 2 h, (orange) = after 6 h, and (grey) = after 24 h.

In Figures 5 and 6, the adsorption and photocatalytic activity of the samples are represented for MG and DBV removal. Similar tendencies are obtained for both pollutants and so are described in the same paragraph. It is to remind that MG is a compound mainly used as dye or pesticide [21] and DBV is a molecule used as textile dye [22].

From Figures 5a and 6a, a high adsorption capacity of the clays and hybrid materials are noticed. Indeed, after 2 h of adsorption, more than 95 % of both molecules are adsorbed showing that clay has a high affinity for both dyes. Only the pure ZnO (at both concentrations) and Clay/ZnO samples do not totally adsorb the two pollutants after 24 h of experiments. Indeed, 80, 37 and 50 % of MG are adsorbed on pure ZnO (1 g/L), pure ZnO (0.3 g/L) and Clay/ZnO respectively after 24 h. For DBV, 73, 25 and 42 % are adsorbed respectively.

So for both materials, the photocatalytic degradation is necessary to eliminate 100 % of the molecules from the water. It is represented on Figures 5b and 6b, in this case the elimination is due to adsorption

and degradation simultaneously. After 24 h of illumination, both molecules are eliminated on both materials. It illustrated the advantage to have a hybrid material that can combine multiple properties to degrade various molecules depending on their resistance to one process to another. As for the PNP degradation, the degradation of the hybrid materials (Figures 5b and 6b) is higher than the ZnO at the concentration of 0.3 g/L, it can be explained by the specific morphology observed with SEM (Figure 3) showing that the ZnO particles are distributed at the surface of clay sheet allowing a very good contact between the pollutant and the photocatalytic material.

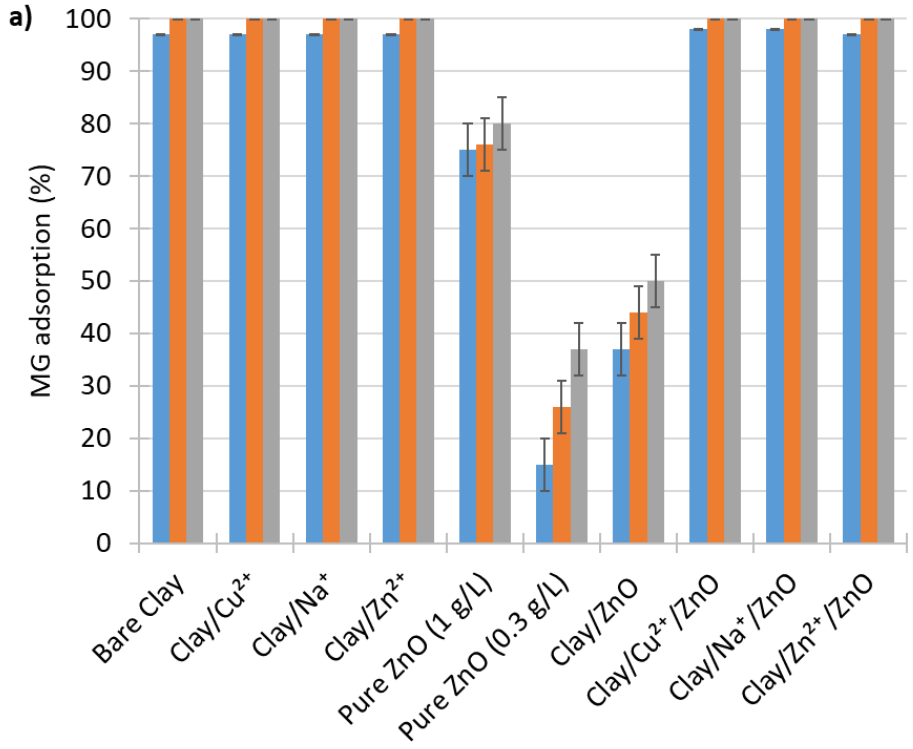

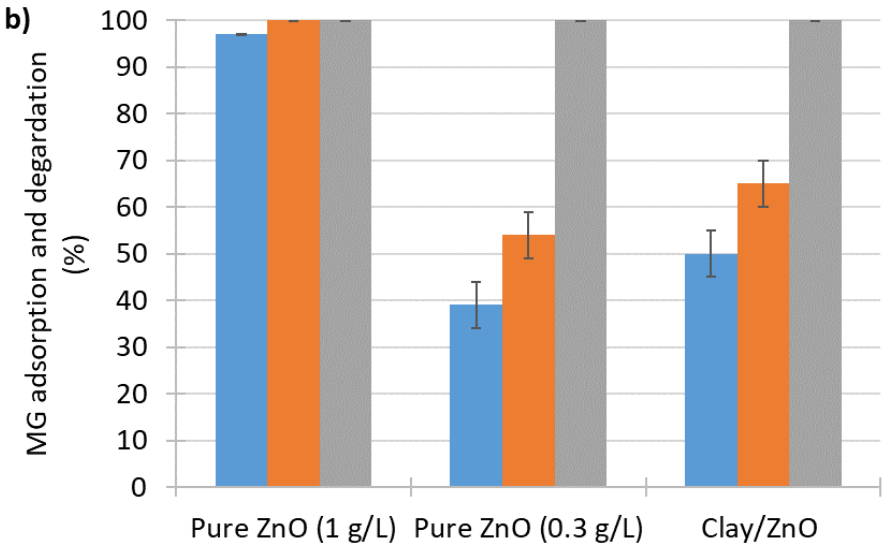

290

291 **Figure 5: (a) MG adsorption and (b) degradation (%) under UVA illumination for 2, 6, and 24 h with**

292 **all samples. (blue) = after 2 h, (orange) = after 6 h, and (grey) = after 24 h.**

293

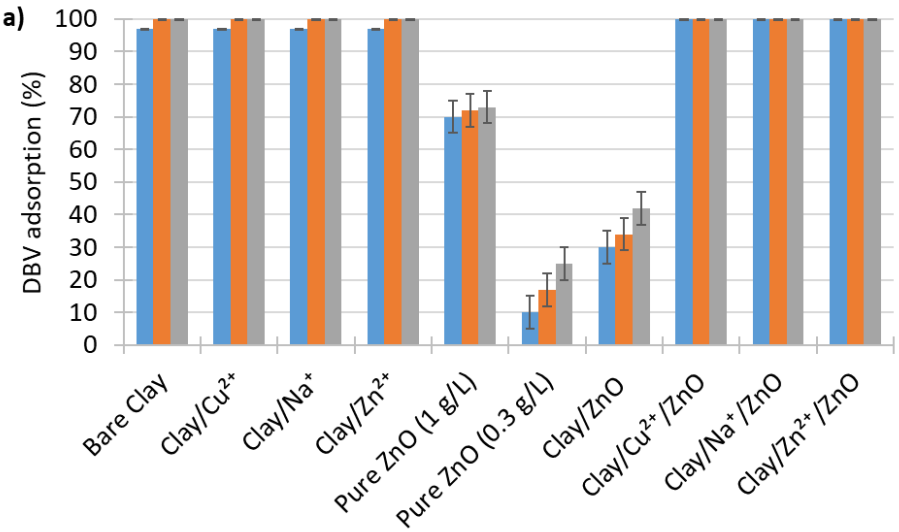

294

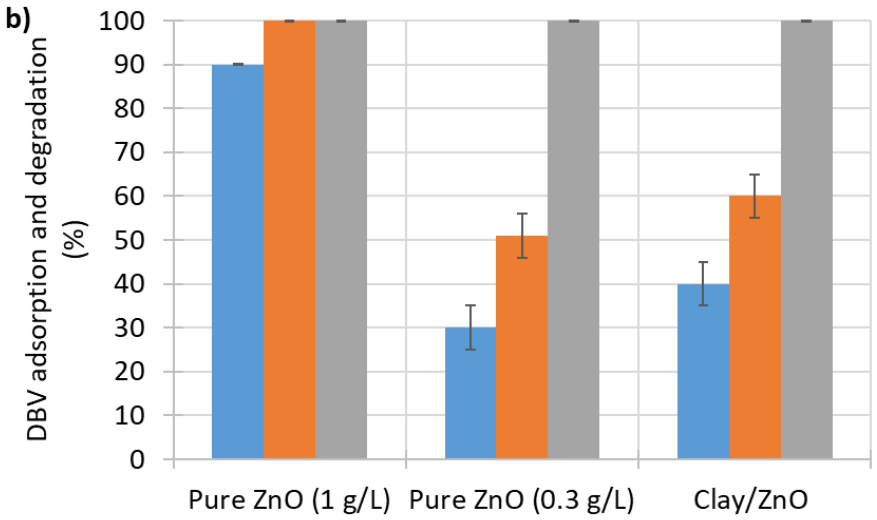

Figure 6: (a) DBV adsorption and (b) degradation (%) under UVA illumination for 2, 6, and 24 h with all samples. (blue) = after 2 h, (orange) = after 6 h, and (grey) = after 24 h.

Thanks to these pollutant removal experiments; the hybrid materials showed their versatile properties for the elimination of different kinds of molecule throughout the adsorption and/or the photocatalytic degradation of these molecules.

If the affinity between the pollutant and the solid is high, high adsorption occurs and the pollutant is removed from the water fixed on the solid. When the affinity is low, the photocatalytic property is needed to degrade the pollutant and treat the water. In this study, MG and DBV have a high affinity for the hybrid materials and are mainly removed by adsorption while PNP has no affinity for the hybrid materials and is totally degraded thanks to the photocatalytic property bring by the ZnO. These different adsorption behaviors are due to the 3 molecules which have different surface groups that can interact differently with the material surface.

4. Conclusions

In this work, natural clay extracted from Cameroon was modified with different ions by the exchange process. These latter were modified with a photocatalytic semiconductor, ZnO. The goal was to produce efficient hybrid materials for pollutant removal in water thanks to adsorption and/or photocatalytic processes. The ZnO that composed the hybrid material was produced by green sol-gel synthesis, a pure sample of ZnO was also produced for comparison purpose. The hybrid materials were synthesized in soft conditions of low temperature and low pressure.

The XRD results showed that the clay belonged to the smectite family and was composed of different crystalline phases as augite, cristobalite, montmorillonite, illite, kaolinite, feldspar, and talc. The pure ZnO was made of wurtzite phase. When the hybrid materials were produced, mix crystalline patterns were obtained with both smectite and wurtzite phases. The ICP-AES analysis showed that similar ratio between ZnO and clay were obtained for the 4 hybrid materials (30 wt.% of ZnO and 70 wt.% of clay). Specific surface areas were obtained for all samples in the range of 30-60 m^2/g with porous volumes evolving from 0.07 to 0.44 cm^3/g.

The SEM observation of the samples had shown that the hybrid materials had the clay structure as skeletal structure (sheet like structure) with the ZnO spherical particles grafted at the surface, giving a good exposure to light to maintain the photocatalytic property.

Then, the pollutant removal property of the samples was evaluated on three different model pollutants: PNP, MG and DBV. On PNP, no adsorption was observed, and photocatalytic property is necessary to eliminate this molecule. With the best hybrid material (Clay/Cu^{2+}/ZnO sample), 80 % of PNP degradation is observed after 6 h of illumination. On MG and DBV, similar behavior was observed. Indeed, the clays and three out of four hybrid materials adsorbed completely both pollutant after 2 h of contact. Only pure ZnO and Clay/ZnO samples needed illumination to degrade completely both molecules. Synergistic effect is observed when the clay is modified by ZnO concerning the photocatalytic degradation activity.

This work showed the possibility to obtain very efficient hybrid materials for pollutant removal in waste waters with the use of inexpensive natural clay modified with a low amount of catalytic material (ZnO

around 30 wt.%). It opens an innovative way for the development of polluted water treatment process in developing countries with lower cost.

Acknowledgments

Julien G. Mahy and Stéphanie D. Lambert thank the F.R.S.-FNRS for their Postdoctoral Researcher position and Research Director position respectively. Marlène Huguette Tsaffo Mbognou thanks the PACODEL for a doctoral grant. The authors thank the CARPOR platform of the University of Liège and its manager, Dr. Alexandre Léonard, for the nitrogen adsorption–desorption measurements.

J.G.M. is grateful to the Rotary for a District 2160 grant, to the University of Liège and the FNRS for financial support for a postdoctoral stay in INRS Centre Eau, Terre, Environnement in Québec, Canada.

Data Availability Statement

The raw/processed data required to reproduce these findings cannot be shared at this time as these data are part of an ongoing study

Conflict of interest

The authors declare that there is no conflict of interest concerning this work.

Ethical Approval

The authors declare that they have no known competing financial interests or personal relationships that could have appeared to influence the work reported in this paper

Consent to Participate

All authors agreed to participate to this work

Consent to Publish

All authors agreed to this version for publication

Authors Contributions

Marlène Huguette Tsaffo Mbognou: Conceptualization, Methodology, Writing – review & editing, Investigation, Formal analysis, Writing – original draft. Stéphanie D. Lambert: Conceptualization, Methodology, Writing – original draft, Writing – review & editing, Funding acquisition, Project administration. Joachim Caucheteux: Investigation, Formal analysis. Antoine Fracy: Investigation, Formal analysis. Christelle Alié: Investigation, Formal analysis. Nathalie Fagel: Supervision, Funding acquisition, Project administration. Emmanuel Djoufac Woumfo: Supervision, Funding acquisition, Project administration. Julien G. Mahy: Conceptualization, Methodology, Writing – original draft, Writing – review & editing, Investigation, Formal analysis, Supervision, Funding acquisition, Project administration.

Funding

This research was funded by PACODEL/University of Liège, bourse de mobilité doctorale.

References

Kemgang Lekomo Y, Mwebi Ekengoue C, Douola A, et al (2021) Assessing impacts of sand mining on water quality in Toutsang locality and design of waste water purification system. Clean Eng Technol 2:. https://doi.org/10.1016/j.clet.2021.100045

Auriol M, Filali-Meknassi Y, Dayal Tyagi R (2007) Présence et devenir des hormones stéroïdiennes dans les stations de traitement des eaux usées. Occurrence and fate of steroid hormones in wastewater treatment plants. Revue des Sciences de l'Eau 20:89–108

Zaviska F, Drogui P, Mercier G, Blais JF (2009) Advanced oxidation processes for waters and wastewaters treatment: Application to degradation of refractory pollutants. Revue des Sciences de l'Eau 22:535–564. https://doi.org/10.7202/038330ar

Hocine O, Boufatit M, Khouider A (2004) Use of montmorillonite clays as adsorbents of hazardous polluants. Desalination 167:141–145. https://doi.org/10.1016/j.desal.2004.06.122

Srivastava R, Fujita S, Arai M (2009) Synthesis and adsorption properties of smectite-like materials prepared using ionic liquids. Appl Clay Sci 43:1–8. https://doi.org/10.1016/j.clay.2008.06.015

Akçay G, Kilinç E, Akçay M (2009) The equilibrium and kinetics studies of flurbiprofen adsorption onto tetrabutylammonium montmorillonite (TBAM). Colloids Surf A Physicochem Eng Asp 335:189–193. https://doi.org/10.1016/j.colsurfa.2008.11.009

Mahy JG, Wolfs C, Mertes A, et al (2019) Advanced photocatalytic oxidation processes for micropollutant elimination from municipal and industrial water. J Environ Manage 250:. https://doi.org/10.1016/j.jenvman.2019.109561

Mahy JG, Lejeune L, Haynes T, et al (2021) Crystalline ZnO photocatalysts prepared at ambient temperature: Influence of morphology on p-nitrophenol degradation in water. Catalysts 11:. https://doi.org/10.3390/catal11101182

Mahy JG, Tilkin RG, Douven S, Lambert SD (2019) TiO<inf>2</inf> nanocrystallites photocatalysts modified with metallic species: Comparison between Cu and Pt doping. Surfaces and Interfaces 17:. https://doi.org/10.1016/j.surfin.2019.100366

Douven S, Mahy JG, Wolfs C, et al (2020) Efficient N, Fe Co-doped TiO2 active under cost-effective visible LED light: From powders to films. Catalysts 10:. https://doi.org/10.3390/catal10050547

Bodson CJ, Heinrichs B, Tasseroul L, et al (2016) Efficient P- and Ag-doped titania for the photocatalytic degradation of waste water organic pollutants. J Alloys Compd 682:144–153. https://doi.org/10.1016/j.jallcom.2016.04.295

Pignatello JJ, Oliveros E, MacKay A (2006) Advanced oxidation processes for organic contaminant destruction based on the fenton reaction and related chemistry. Crit Rev Environ Sci Technol 36:1–84. https://doi.org/10.1080/10643380500326564

Issaka E, AMU-Darko JNO, Yakubu S, et al (2022) Advanced catalytic ozonation for degradation of pharmaceutical pollutants—A review. Chemosphere 289:. https://doi.org/10.1016/j.chemosphere.2021.133208

Mahy JG, Tasseroul L, Zubiaur A, et al (2014) Highly dispersed iron xerogel catalysts for p-nitrophenol degradation by photo-Fenton effects. Microporous and Mesoporous Materials 197:164–173. https://doi.org/10.1016/j.micromeso.2014.06.009

Hu Z, Cai J, Song G, et al (2021) Anodic oxidation of organic pollutants: Anode fabrication, process hybrid and environmental applications. Curr Opin Electrochem 26:. https://doi.org/10.1016/j.coelec.2020.100659

Drogui P, Blais J-F, Mercier G (2007) Review of Electrochemical Technologies for Environmental Applications. Recent Patents on Engineering 1:257–272

Cheng T, Gao H, Liu G, et al (2022) Preparation of core-shell heterojunction photocatalysts by coating CdS nanoparticles onto Bi4Ti3O12 hierarchical microspheres and their photocatalytic removal of organic pollutants and Cr(VI) ions. Colloids Surf A Physicochem Eng Asp 633:. https://doi.org/10.1016/j.colsurfa.2021.127918

Xiong S, Yin Z, Zhou Y, et al (2013) The dual-frequency (20/40 kHz) ultrasound assisted photocatalysis with the active carbon fiber-loaded Fe3+-TiO2 as photocatalyst for degradation of organic dye. Bull Korean Chem Soc 34:3039–3045. https://doi.org/10.5012/bkcs.2013.34.10.3039

Tang N, Li Y, Chen F, Han Z (2018) In situ fabrication of a direct Z -scheme photocatalyst by immobilizing CdS quantum dots in the channels of graphene-hybridized and supported mesoporous titanium nanocrystals for high photocatalytic performance under visible light. RSC Adv 8:42233–42245

Mahy JG, Lambert SD, Tilkin RG, et al (2019) Ambient temperature ZrO<inf>2</inf>-doped TiO<inf>2</inf> crystalline photocatalysts: Highly efficient powders and films for water depollution. Mater Today Energy 13:. https://doi.org/10.1016/j.mtener.2019.06.010

Alderman DJ (1985) Malachite green: a review. J Fish Dis 8:289–298

Lalonger L (1994) La transition des colorants naturels aux colorants synthétiques et ses répercussions. Material Culture Review 40:

Mahy JG, Mbognou MHT, Léonard C, et al (2022) Natural Clay Modified with ZnO/TiO2 to Enhance Pollutant Removal from Water. Catalysts 12:. https://doi.org/10.3390/catal12020148

Benhebal H, Chaib M, Crine M, et al (2016) Photocatalytic decolorization of gentian violet with Na-doped (SnO2 and ZnO). Chiang Mai Journal of Science 43:584–589

Benhebal H, Chaib M, Leonard A, et al (2012) Photodegradation of phenol and benzoic acid by sol-gel-synthesized alkali metal-doped ZnO. Mater Sci Semicond Process 15:264–269. https://doi.org/10.1016/j.mssp.2011.12.001

Mahy JG, Lambert SD, Léonard GLM, et al (2016) Towards a large scale aqueous sol-gel synthesis of doped TiO2: Study of various metallic dopings for the photocatalytic degradation of p-nitrophenol. J Photochem Photobiol A Chem 329:189–202. https://doi.org/10.1016/j.jphotochem.2016.06.029

Ndé HS, Tamfuh PA, Clet G, et al (2019) Comparison of HCl and H2SO4 for the acid activation of a cameroonian smectite soil clay: palm oil discolouration and landfill leachate treatment. Heliyon 5:. https://doi.org/10.1016/j.heliyon.2019.e02926

Theo Kloprogge J, KOMARNENl S, Amonetie JE (1999) SYNTHESIS OF SMECTITE CLAY MINERALS: A CRITICAL REVIEW. Clays Clay Miner 47:529–554

Seo YJ, Seol J, Yeon SH, et al (2009) Structural, mineralogical, and rheological properties of methane hydrates in smectite clays. J Chem Eng Data 54:1284–1291. https://doi.org/10.1021/je800833y

Pirhashemi M, Habibi-Yangjeh A, Rahim Pouran S (2018) Review on the criteria anticipated for the fabrication of highly efficient ZnO-based visible-light-driven photocatalysts. Journal of Industrial and Engineering Chemistry 62:1–25. https://doi.org/10.1016/j.jiec.2018.01.012

Rauf MA, Meetani MA, Hisaindee S (2011) An overview on the photocatalytic degradation of azo dyes in the presence of TiO2 doped with selective transition metals. Desalination 276:13–27. https://doi.org/10.1016/j.desal.2011.03.071

Romero V, Acevedo S, Marco P, et al (2016) Enhancement of Fenton and photo-Fenton processes at initial circumneutral pH for the degradation of the β-blocker Metoprolol. Water Res 88:449–457. https://doi.org/http://dx.doi.org/10.1016/j.watres.2015.10.035

Lin SS, Lu JG, Ye ZZ, et al (2008) p-type behavior in Na-doped ZnO films and ZnO homojunction light-emitting diodes. Solid State Commun 148:25–28. https://doi.org/10.1016/j.ssc.2008.07.028